First-principles study of the band structure and optical absorption of $CuGaS_2$

Irene Aguilera,[1,2,3] Julien Vidal,[2,3,4] Perla Wahnón,[1] Lucia Reining,[2,3] and Silvana Botti[2,3,5,*]

[1]*Instituto de Energía Solar and Departamento de Tecnologías Especiales, ETSI Telecomunicación, UPM, Ciudad Universitaria, ES-28040 Madrid, Spain*

[2]*Laboratoire des Solides Irradiés (LSI), École Polytechnique, CNRS, CEA-DSM, F-91128 Palaiseau, France*

[3]*European Theoretical Spectroscopy Facility (ETSF)*

[4]*Institute for Research and Development of Photovoltaic Energy (IRDEP), UMR 7174 CNRS/EDF/ENSCP, 6 Quai Watier, F-78401 Chatou, France*

[5]*Laboratoire de Physique de la Matière Condensée et Nanostructures (LPMCN), Université "Claude Bernard" Lyon 1, CNRS, Domaine Scientifique de la Doua, F-69622 Villeurbanne, France*

(Received 13 January 2011; revised manuscript received 19 April 2011; published 30 August 2011)

$CuGaS_2$ is the most promising chalcopyrite host for intermediate-band thin-film solar cells. Standard Kohn-Sham density functional theory fails in describing the band structure of chalcopyrite materials, due to the strong underestimation of the band gap and the poor description of *p-d* hybridization, which makes it inadvisable to use this approach to study the states in the gap induced by doping. We used a state-of-the-art restricted self-consistent *GW* approach to determine the electronic states of $CuGaS_2$: in the energy range of interest for optical absorption, the *GW* corrections shift the Kohn-Sham bands almost rigidly, as we proved through analysis of the effective masses, bandwidths, and relative position of the conduction energy valleys. Furthermore, starting from the *GW* quasiparticle bands, we calculated optical absorption spectra using different approximations. We show that the time-dependent density functional theory can be an efficient alternative to the solution of the Bethe-Salpeter equation when the exchange-correlation kernels derived from the Bethe-Salpeter equation are employed. This conclusion is important for further studies of optical properties of supercells including dopants.

DOI: 10.1103/PhysRevB.84.085145 PACS number(s): 71.10.−w, 71.15.Mb, 71.15.Qe, 78.20.Ci

I. INTRODUCTION

In the quest of lower-cost solar cells, the thin-film approach has been proposed to cut the costs associated with the absorber by reducing the volume of material required. In this context, Cu-based chalcopyrite semiconductors of the form $Cu(Ga,In)(S,Se)_2$ (CIGS) appear to be one of the most promising thin-film alternatives to silicon.[1] Compounds belonging to the CIGS family exhibit structural, optical, and electrical properties that can be, in principle, tuned as a function of the composition (presence of native defects) and the growth process. In addition, this class of semiconductors possesses direct band gaps and high optical absorption coefficients, which allows us to reduce to a few microns the thickness necessary to capture all the incoming photons with a frequency higher than the band gap. In addition to the decrease in the cost of the absorber material, this improves the efficiency of the devices, as higher absorption leads to a higher photocurrent. Thin-film chalcopyrite technology is thus nowadays a solid candidate for second-generation photovoltaics, with the highest efficiency among thin-film solar cells (20.1%).[2]

All chalcopyrite CIGS unit cells present an internal distortion with respect to the standard zincblende lattice, since the existence of two different cations (Cu, In) results in two different bonding lengths between cations and anions.[3] The anion displacement parameter u measures this distortion of the (S,Se) sublattice. It is well known that the value of u has a large influence on the band gap of CIGS chalcopyrites.[3–6]

The experimental band gaps of CIGS range from 1.05 eV for $CuInSe_2$[7] to around 2.5 eV for $CuGaS_2$.[8] This work is devoted to the study of the latter, which has an experimental optical gap of 2.4–2.5 eV[8] at room temperature, obtained from electroreflectance spectra, and 2.53 eV at 0 K,[9–12] obtained from photoreflectance and absorption spectra. One should keep in mind when comparing calculated quasiparticle (QP) energy bands and optical data that the QP (or photoemission) and optical gaps differ by the exciton binding energy (<0.05 eV for $CuGaS_2$).[11]

According to the Shockley-Queisser limit,[13] the maximum efficiency for solar cells based on *p-n* junctions can be obtained for a band gap of 1.4 eV. $CuGaS_2$ should therefore be ruled out as an absorber for single-junction cells.[14] On the other hand, thanks to its wide gap, $CuGaS_2$ is currently used as a window layer for photovoltaic applications. However, the main interest of this compound lies in the possibility of hosting a narrow intermediate band inside the band gap, when it is highly doped with transition metals (such as Ti or Cr).[15–17] In 1997, it was shown[18] that a significant increase in the efficiency of solar cells could be obtained by introducing impurity energy levels in the semiconductor band gap that absorbs additional lower energy photons. It was proposed, and recently observed experimentally,[19] that when the concentration of impurities is high enough to give rise to a band (the intermediate band), nonradiative recombination can be suppressed, leading to theoretical efficiencies much higher than those of a conventional solar cell. Since the theoretical optimal value of the band gap for a thin-film host semiconductor for intermediate-band photovoltaic applications is around 2.4 eV,[20] $CuGaS_2$ is the ideal chalcopyrite host.[14–17] Moreover, $CuGaS_2$ was the first semiconductor proposed to combine the intermediate-band concept and the thin-film technology.

Regarding the optical properties of $CuGaS_2$, some experimental[7,10,11,21,22] and theoretical[23–25] studies in the visible range have been reported so far. The excitonic peak in the optical spectra has been characterized only

experimentally.[10,21,26,27] Moreover, experimental results are not always easy to interpret, in particular, as there are large discrepancies among them. From the theoretical side, and despite many efforts, calculations in the literature are not accurate enough to help in the understanding of experimental measurements. Indeed, the main problem comes from the fact that the $CuGaS_2$ electronic states close to the energy gap arise from the hybridization of the d states of Cu with the p states of S. This leads to subtle exchange and correlation effects that are very hard to take into account using standard density functionals. As a result, the p-d hybridization is overestimated.[28] The *ab initio* results published up to now were obtained from density functional theory (DFT),[29,30] based either on the local density approximation (LDA) or on generalized gradient approximations (GGAs). However, DFT is hampered by two important shortcomings when applied in this context: (i) the Kohn-Sham (KS) band gap is systematically underestimated by 50% to 100% compared to photoemission experiments; and (ii) there is deficient cancellation of the spurious self-interaction terms in standard functionals, particularly critical for d electrons, which are usually located too high in energy. For systems with shallow d states, like the chalcopyrites, this has a direct effect on the band gap.

It is clear that, in order to predict correctly both band gaps and optical absorption spectra, it is necessary to go beyond standard KS DFT methods. Many-body perturbation theory (MBPT), in particular, the GW approximation[31] for QP states and the subsequent solution of the Bethe-Salpeter equation (BSE),[32] have yielded electronic properties in very good agreement with experiments for a wide range of materials.[33–39] In the MBPT scheme, the QP wave functions φ_i and energies ε_i satisfy the Schrödinger-like equation

$$[-\nabla^2/2 + V_{\text{ext}}(\mathbf{r}) + V_{\text{H}}(\mathbf{r})]\varphi_i(\mathbf{r}) + \int \Sigma(\mathbf{r},\mathbf{r}';\varepsilon_i)\varphi_i(\mathbf{r}')d^3r' = \varepsilon_i\varphi_i(\mathbf{r}), \quad (1)$$

where V_{ext} is the external (pseudo)potential due to the ions, V_{H} is the classical Hartree potential, and the self-energy Σ contains all the effects of exchange and correlation among electrons.

In the GW approximation[31] the self-energy is written as the product

$$\Sigma_{GW}(1,2) = iG(1,2)W(1^+,2), \quad (2)$$

where $G(1,2)$ is the one-particle Green's function of the system and $W(1^+,2)$ the dynamically screened Coulomb interaction. The argument 1 stands for (r_1,σ_1,t_1) and 1^+ means that the limit $t_1 + \eta \to t_1$ should be taken for η positive. Usually, Eq. (1) is solved in the perturbative G_0W_0 scheme, where G and W are calculated directly from LDA eigenvalues and eigenfunctions, while the QP corrections to LDA eigenvalues are evaluated as a first-order perturbation. Applying the G_0W_0 approach gives very good results for many materials.[34] However, it has been shown that it fails for compounds with d electrons,[35,36] especially when d states hybridize with p states close to the Fermi energy.[6,40–42] When G_0W_0 fails, a self-consistent (sc) scheme or better starting points are the possible ways to obtain accurate electronic bands.

In the present work, we use a simplified scGW scheme based on Hedin's Coulomb hole and screened exchange (COHSEX) approximation,[31] followed by a perturbative G_0W_0 step. The COHSEX is a static and Hermitian approximation to the GW self-energy. scCOHSEX leads to band gaps that are usually too large. The final step of our method, the perturbative G_0W_0 performed on top of the scCOHSEX iterations, accounts for the dynamical screening that is missing in the COHSEX approximation, yielding QP energies in excellent agreement with experiments.[6,35,40] Moreover, scCOHSEX wave functions were found[35] to be very similar to those obtained by applying the original QP scGW scheme (QPscGW) of Faleev *et al.*[43] Besides being in good agreement with both experiments and QPscGW results, the scCOHSEX + G_0W_0 scheme is computationally less expensive, as it involves only sums over occupied states to build the self-energy matrix elements.

Standard KS DFT is inadequate for the accurate prediction of electronic excitations. To calculate optical spectra one has to deal with neutral excitations due to the simultaneous creation of a quasielectron and a quasihole which interact in the system. A possible way to go beyond the application of Fermi's golden rule, which is a simple sum over independent transitions between KS states, is to use the time-dependent (TD) generalization of DFT (TDDFT),[44,45] where the electronic density responds to a TD external field. TDDFT retains all the advantages of the DFT formalism in terms of computational efficiency. However, the lack of good approximations for the TD exchange-correlation (xc) functional (especially in the case of solids)[38,39] is its principal limitation.

The xc kernel (f_{xc}) of TDDFT, which is the variation of the xc potential with respect to the electronic density, is most often approximated by (i) $f_{\text{xc}} = 0$, leading to the random-phase approximation (RPA), or (ii) $f_{\text{xc}} = \delta v_{\text{xc}}^{\text{LDA}}/\delta\rho$, which gives the adiabatic LDA[45,46] (ALDA). Note that the RPA differs from an independent-particle calculation, even if the xc kernel is 0, because it accounts for variations of the Hartree potential upon excitation. This is a classical contribution, which, in the optical spectra, corresponds to local field or depolarization effects, particularly important when charge inhomogeneities are pronounced.

Concerning the calculation of absorption spectra of semiconductors, neither the RPA nor the ALDA is sufficient to yield results in quantitative (and sometimes not even in qualitative) agreement with experiments. Nevertheless, it has been shown[39,47] that in some cases an agreement with experiments can be recovered within TDDFT by retaining only the long-range contribution (LRC) that the exact f_{xc} should have in the asymptotic limit. This model kernel accounts for continuum excitonic effects, giving very good optical properties for small- to medium-gap semiconductors, with a computational burden comparable to a DFT approach.

Two forms for this LRC kernel are used in this work: a static[47,48] form given by $-\alpha^{\text{static}}/q^2$ and its dynamical extension[49] $-(\alpha^{\text{dyn}} + \beta\omega^2)/q^2$, where α^{static}, α^{dyn}, and β are parameters that can be calculated from the knowledge of the static dielectric constant and the plasma frequency of the material.[48,49] One should remember, however, that $CuGaS_2$ possesses bound excitons[10,21,26,27] and that the TDDFT-LRC approach has proved to work better for systems with continuum excitons. That is why in this case it is worth resorting

to solution of the computationally demanding BSE, which accurately describes the electron-hole pair dynamics. Indeed, applications of BSE to several materials have been reported in the literature,[38,39] with excellent agreement with experiments.

In the following we present results for the electronic band structure (Sec. III) and optical absorption spectra (Sec. IV) of $CuGaS_2$ that we obtained by applying the above-described hierarchy of *ab initio* schemes. We carried out similar calculations for the other members of the CIGS family and the results are strictly analogous, as a consequence of the fact that in all CIGS compounds the physics of the band gap is controlled by the *p*-*d* hybridization of the top valence states.

On one hand, our results allow us to assess the validity of different approximations and calculation schemes for the determination of electronic and optical properties of Cu-based chalcopyrite materials. Our aim is to determine how to obtain sufficiently accurate results using the most efficient approaches, in order to lay the basis for tackling, in the near-future, the more complex problem of studying the optical absorption of $CuGaS_2$ doped with transition metals. One should remember that scGW calculations and the solution of the BSE are too computationally demanding at present in order to be applied systematically for large supercells made of atoms with many valence electrons.

Moreover, comparison of the most accurate calculations with available experimental data for $CuGaS_2$ is used to analyze the origin of spectral features and clarify the existing discrepancies among experimental results. Our conclusions are summarized in Sec. V.

II. COMPUTATIONAL DETAILS

All electronic-structure calculations were performed using the first-principles code ABINIT.[35,50–52] We first generated and tested *ab initio* norm-conserving pseudopotentials,[53] obtained within the Troullier-Martins[54] and the Hamann[55] schemes using the code FHI98PP.[56] The electronic ground state was calculated using DFT within the LDA approximation of Perdew and Wang[57] for the xc functional. LDA eigenstates were used as a starting point for either G_0W_0 or scCOHSEX calculations. In the case of G_0W_0, the convolution in the Fourier transform of Eq. (2) was performed using a plasmon-pole model for the frequency dependence of the dielectric function.[58]

In this work we used the fully relaxed primitive cell and the internal coordinates obtained within the DFT-LDA. The relaxed structural parameters ($a = 5.3819$ Å, $c = 10.66$ Å) are in agreement with experimental data within less than 2%. The relaxed anion displacement u is equal to 0.2581, compared to an experimental range of [0.25–0.275].[59–62] Note that in the case of $CuIn(S,Se)_2$, the LDA and GGA gave a value of u outside the experimental window.[6] We verified that this does not happen when dealing with $CuGaS_2$ and $CuGaSe_2$.

It is known[63] that for GW calculations special care must be taken in the choice of the pseudopotential core-valence partitions. When the core and valence electrons are separated in the procedure to build a pseudopotential, the self-energy has a contribution from the core-valence exchange interaction, which is treated at the LDA level if the semicore states belong to the core. For this reason, GW corrections can contain a substantial error when the spatial overlap between the valence and the semicore wave functions is sizable. This fact led in the past to some claims[64] concerning the failure of the pseudopotential approach for GW calculations. However, it has been proved[65–67] that when semicore states are included in the valence GW results are reliable.

In our calculations this problem appears, as *d* electrons have to be taken into account explicitly in the pseudopotential, as in the case of Cu or Ga. In the case of Cu, it has been shown that it is crucial to take the whole shell in the valence[68,69] in order not to obtain unphysical GW corrections. Marini *et al.*[68] proved that this behavior is due to the fact that Cu $3s$ and $3p$ states, despite being well separated in energy from the $3d$ ones, have a large spatial overlap with the latter. As a consequence, non-negligible contributions to the self-energy come from the exchange contributions between $3d$ and $3s$-$3p$ states. Similar conclusions were reached by Bruneval *et al.*,[69] who showed that if Cu semicore states are included in the core, the GW approximation predicts wrongly Cu_2O to be metallic.

As a consequence of the selected core-valence partition, the kinetic energy cutoff used to describe the electronic density and the wave functions becomes rather high (between 80 and 130 Ha, depending on the choice made for the Ga pseudopotential). While the valence-band maximum (VBM) in $CuGaS_2$[4] has a considerable Cu $3d$ character, the necessity for the inclusion of Ga $3d$ states in the valence is less obvious due to their high binding energies (19.85 eV with respect to the VBM).[70] Note, moreover, that the generation of reliable Ga pseudopotentials has been a challenge for many years.[71] To shed light on this issue, we tested two different Ga pseudopotentials: one, which we refer to as the Ga pseudopotential without a semicore, has three valence electrons ($4s^24p^1$), while the other also includes $3d^{10}$, $3s^2$, and $3p^6$ electrons in the valence (Ga pseudopotential with semicore). To evaluate the effect of the inclusion of semicore states in the Ga pseudopotential, we calculated the band structure of $CuGaS_2$ and, in particular, the value of the band gap using the two Ga pseudopotentials with a different number of valence electrons. We observed that the band dispersions were very similar, independently of which pseudopotential we used, and there were only discrepancies as small as 0.1 eV in the value of the QP band gap yielded by G_0W_0, and scCOHSEX + G_0W_0 calculations. Only the strongly underestimated KS LDA band gap showed a larger discrepancy (0.25 eV). We concluded therefore that using the Ga pseudopotential without a semicore would not significantly affect the accuracy of our GW results. More precisely, we estimate that our energy levels have an error bar of 0.1–0.2 eV, which is comparable to the difference between experimental results. In view of this, we decided to use in the following the Ga pseudopotential with only three valence electrons. This choice is particularly attractive for limiting the computational effort as much as possible, especially in view of the fact that the application of $CuGaS_2$ as an intermediate-band host requires the construction of supercells including doping.

The number of bands used in the sums over states for the calculations of W and G was 250 and 200, respectively. Furthermore, the following energy cutoffs of the plane-wave basis were necessary to converge eigenvalues with a

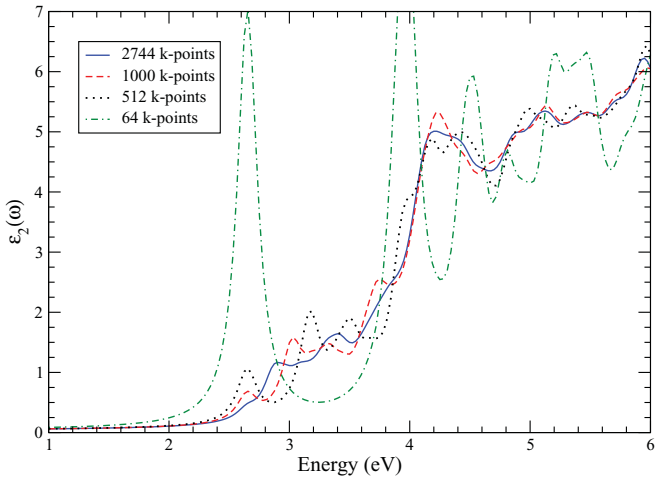

FIG. 1. (Color online) Convergence of the RPA absorption spectrum with respect to the density of the **k**-point grid.

tolerance of less than 20 meV for calculations with the Ga pseudopotential without a semicore: 80 Ha for the KS wave functions, 50 Ha for the wave functions used to calculate W, 15 Ha for the size of the W matrix in reciprocal space, and 70 Ha for the wave functions used to calculate Σ and for the size of the Σ_x matrix in reciprocal space. For calculations with the Ga pseudopotential with a semicore, note that the inclusion of the shell $n = 3$ in the valence of the Ga pseudopotential leads to a significant increase in the kinetic energy cutoffs. Approximately a double number of plane waves was thus necessary for convergence in the case of this pseudopotential.

In the sc cycles, the COHSEX wave functions were represented on a restricted LDA basis set, with 59 and 42 LDA bands for calculations with the Ga pseudopotential with and without a semicore, respectively. A Monkhorst-Pack **k**-point mesh of $3 \times 3 \times 3$ was used to sample the Brillouin zone for GW calculations. This corresponds to 6 **k** points in the irreducible wedge of the Brillouin zone and 27 **k** points in the full Brillouin zone.

Calculations of the optical spectra were performed using the code YAMBO.[72] To get a well-converged RPA dielectric function, a $14 \times 14 \times 14$ shifted grid was needed to sample the Brillouin zone. This corresponds to 2744 **k** points in the full Brillouin zone. Moreover, 20 empty bands were needed to reach convergence in the range of photon energies from 0 to 6 eV.

The solution of the BSE is computationally heavier than an RPA or ALDA calculation using TDDFT; for this reason, we could not use a $14 \times 14 \times 14$ shifted grid of **k** points. A $10 \times 10 \times 10$ shifted grid (which gives 1000 **k** points) yields a spectrum where the relevant peaks are already well defined, despite the presence of spurious wiggles due to the finite **k**-point sampling. Since a similar convergence issue is present in the RPA calculations, we show in Fig. 1 the slow convergence with respect to the number of **k** points of the RPA absorption spectrum. An analogous convergence issue was already detected in previous works.[73] In this case, it is determined by the strong dispersion of the first conduction band close to Γ. Nevertheless, one can see that a mesh of 1000 shifted **k** points is clearly sufficient to determine the peak position with a precision of 0.1 eV. In fact, many approximations are involved in the various steps of our calculations and we can expect an accuracy of the order of 0.1 eV in the position of our peaks. Once the peak position and relative intensity of the peaks do not evolve any more (as proven in Fig. 1) by increasing the number of **k** points, the presence of some residual wiggles is acceptable, as long as one keeps their origin in mind.

III. QUASIPARTICLE BAND STRUCTURES

The band gaps of $CuGaS_2$ obtained using the different theoretical approaches are summarized in Table I. As mentioned above, the standard G_0W_0 approach fails for chalcopyrites because the DFT-LDA states are not a good starting point for a simple perturbative correction of the eigenenergies. As a result, the G_0W_0 band gap (1.34 eV) is still far from the experimental one (2.4–2.53 eV). When a perturbative G_0W_0 fails, accurate band gaps can be obtained moving away from the DFT starting point, using, e.g., a restricted sc scheme. Self-consistency using the COHSEX approximation for the self-energy leads, as usual, to a band gap that is too large (3.29 eV). The inclusion of dynamical effects through a perturbative G_0W_0 step on top of scCOHSEX corrects the result: the difference between experiment and scCOHSEX + G_0W_0 is about 0.1 eV. In fact, we remind the reader that the experimental measurements

TABLE I. Theoretical and experimental band gaps E_g and binding energies of the valence states compared to XPS results. All energies are given in electron volts with respect to the valence band maximum. Results for the Ga 3d binding energy are taken from the calculation done using the Ga pseudopotential with a semicore.

	LDA	G_0W_0	scCOHSEX	scCOHSEX + G_0W_0	Expt.
E_g	0.70	1.34	3.29	2.65	2.4–2.53[a]
Cu 3d + S 3p					
First peak	1.5	1.4	1.8	1.7	1.6,2.1[b]
Second peak	3.2	3.3	3.6	3.6	3.4[b]
Ga-S bond	6.9	7.5	7.6	7.8	7.1[b]
S 3s	12.9	13.2	14.4	14.0	13.0,[b]13.4[c]
Ga 3d	15.3–15.7	17.1–17.2	19.2–19.5	19.4–19.6	18.8–19.3,[b]19.85[c]

[a]From Refs. 8, 9, and 12.
[b]From Ref. 74.
[c]From Ref. 70

yield optical gaps, which means that the difference with respect to our calculated QP gap must be decreased by the excitonic binding energy of around 0.05 eV.[11] We also remind that the error due to the neglect of the semicore in the Ga pseudopotential is of the same order.

In Table I we have also gathered the positions of the main peaks of the density of states (DOS) calculated at the different theoretical levels, together with x-ray photoelectron spectroscopy (XPS) results from Refs. 70 and 74. The upper valence band is responsible for two peaks, corresponding to bonding and antibonding of hybridized Cu $3d$ and S $3p$ states. The following group of bands is made of Ga-S bonding states. Then we find S s states and, finally, the d states of Ga.

The width of both theoretical and experimental structures has to be taken into account for the comparison. However, it can be clearly seen that a GW approach improves LDA results, especially when d states are involved. Indeed, for states with d character (Cu $3d$–S $3p$ hybridization and Ga $3d$ states), we expect that LDA wave functions are too delocalized. In particular, for the $3d$ states of Ga (which are obtained from the calculations with the Ga pseudopotential with semicore states in the valence), the scGW approach shifts their position by 4 eV, placing them very close to experimental data. In the case of the Ga-S bonding and S $3s$ states, GW tends to increase the binding energies in the right direction, but leading to a slight overcorrection. It should be noted that for the highest binding energies, the predicted values cannot be considered as accurate as for low binding energies, due to the use of the plasmon-pole model.[75] This issue does not affect the calculations of the optical spectra, as the energy region of interest is close to the Fermi energy.

In Fig. 2 we show the dispersion of LDA and scCOHSEX + G_0W_0 electronic energy bands of $CuGaS_2$. The correction to the band gap within scCOHSEX + G_0W_0 is very large: the direct band gap at Γ goes from 0.7 eV in LDA to 2.65 eV, as a result of a downshift of the valence band edge by 0.67 eV and an upshift of the conduction band edge by 1.28 eV. However, GW corrections are not very sensitive to the **k** point, and therefore the overall dispersion of the bands in LDA and scCOHSEX + G_0W_0 is similar, which justifies the use of a scissor operator to simulate GW corrections in the energy

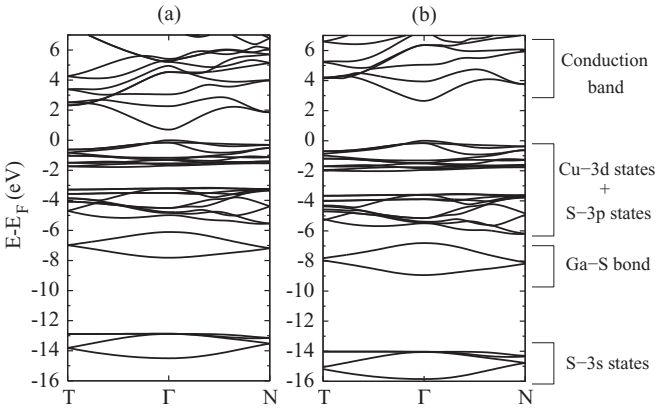

FIG. 2. Band structure of $CuGaS_2$ using (a) the LDA and (b) scCOHSEX + G_0W_0.

window close to the gap. In particular, we observed that the valence band width close to the gap changes by less than 0.1 eV, and analogously, the distance between the conduction valleys at Γ, N, and T changes by less than 0.1 eV. We also evaluated the effective masses at Γ and compared them with previous calculations[76] and experimental data.[11] Our results, summarized in Table II, are in excellent agreement with experiments. Note that we do not include spin-orbit coupling in our calculations. However, it is known that its inclusion is essential to describe the dispersion of the top valence of Se compounds, while it has minor effects on S compounds.

Note that, as in the case of $CuInS_2$,[6] the gap is strongly dependent on the value of the anion displacement u: different values of u within the experimental range [0.25–0.275] can lead to variations of the band gap by 0.4 eV in LDA and 0.8 eV in scCOHSEX + G_0W_0.

In order to verify that the QP wave functions and the LDA ones differ significantly, we analyzed the overlap between LDA and COHSEX wave functions. This overlap is an indication of the variation of COHSEX wave functions with respect to LDA ones. We found that there is a number of states for which the overlap between scCOHSEX and LDA wave functions is significantly smaller than 1 (down to 0.8),

TABLE II. Electron effective masses m_{c1} for the first conduction band at Γ and hole effective masses $m_{v1,v2,v3}$ for the three highest valence states at Γ. All effective masses are given in units of electron mass.

Effective mass	LDA	scGW	GGA + U from Ref. 76	Expt. from Ref. 11
$m_{c1}^{\perp}$	0.13	0.13	0.24	
$m_{c1}^{\parallel}$	0.12	0.12	0.24	
Average m_{c1}	0.13	0.13	0.24	0.12
$m_{v1}^{\perp}$	1.22	0.90	0.91	
$m_{v1}^{\parallel}$	0.16	0.15	0.30	
Average m_{v1}	0.87	0.65	0.70	0.68
$m_{v2}^{\perp}$	5.37	1.60	0.42	
$m_{v2}^{\parallel}$	0.94	0.78	0.82	
Average m_{v2}	3.90	1.33	0.55	1.44
$m_{v3}^{\perp}$	0.16	0.16	0.41	
$m_{v3}^{\parallel}$	0.94	0.78	0.81	
Average m_{v3}	0.42	0.36	0.54	0.39

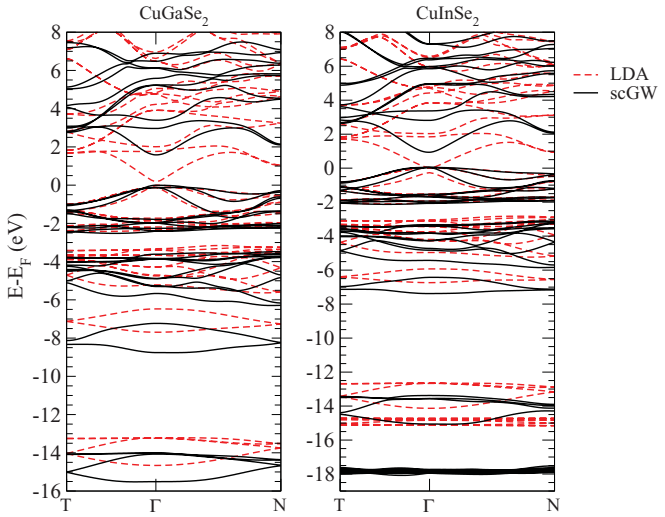

FIG. 3. (Color online) Band structures of $CuGaSe_2$ and $CuInSe_2$ obtained using the LDA [dashed (red) lines] and scCOHSEX + G_0W_0 [solid (black) lines].

signaling a pronounced change in the wave functions due to the sc iterations. The projections are smaller for the more localized states of the valence, which correspond to flatter bands. For these states, the performance of the LDA is worse and so the QP wave functions differ more from the LDA ones. As a matter of fact, the states at the top valence, formed by a *p-d* hybridization, showed the smallest overlaps.

The results we have discussed for the band structure of $CuGaS_2$ can be generalized to all members of the CIGS family, as the physics that determine the band gap is, in all these compounds, the repulsion of antibonding and bonding *p-d* hybridized states. As we can see in Fig. 3, the sc*GW* corrections to the LDA band structures of $CuGaSe_2$ and $CuInSe_2$ are, to a large extent, rigid shifts as in the case of $CuGaS_2$. The band gap correction is more spectacular in $CuInSe_2$, as the LDA gap is negative for the In compounds of the CIGS family: in fact, the top valence band at Γ is located above the lowest conduction state. The correct band ordering is re-established using a *GW* approach.

IV. OPTICAL PROPERTIES

Starting from the KS and *GW* band structures presented in Sec. III, we calculated optical absorption spectra within a linear response, applying TDDFT and solving the BSE. Figures 4 and 5 show calculations of the imaginary part of the macroscopic dielectric function for light polarized along the *c* axis. The theoretical curves are also compared with the experimental data published in Refs. 21 and 74.

The experimental dielectric functions of Alonso *et al.*[7] were obtained with ellipsometry at room temperature, whereas the spectra of Levcenko *et al.*[21] were extracted from reflection spectra measured at 77 K, using the Kramers-Kronig relations. Both results are for single-crystal samples. We can observe that the two curves are rather different. In particular, the absorption spectrum of Levcenko *et al.*[21] has a much lower intensity (about half) than the experimental curve of Alonso *et al.* and previous results of Rife *et al.*[74], probably due to the quality of

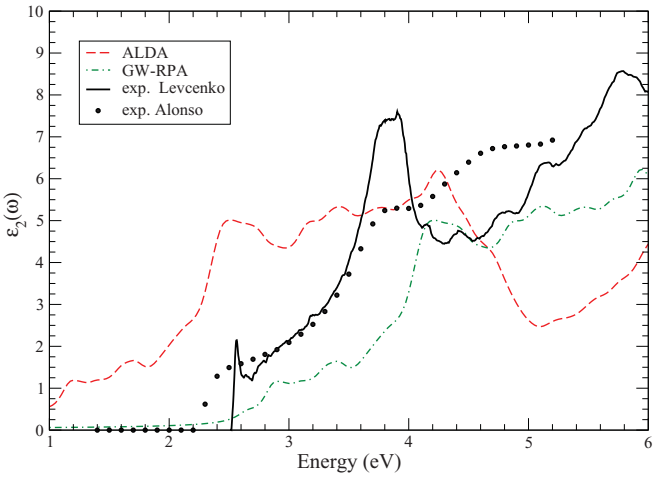

FIG. 4. (Color online) Imaginary part of the dielectric function for light polarized along the *c* axis obtained with TDDFT using the ALDA kernel [dashed (red) line], the RPA using *GW* eigenvalues [dot-dashed (black) line] compared to experimental data of Alonso *et al.*[7] (filled circles) and Levcenko *et al.*[21] [solid (black) line; in arbitrary units; see text].

the reflecting surface of the samples. In view of the above, in all graphs we rescaled the intensity of the absorption spectrum of Levcenko *et al.*[21]

Another discrepancy among the available experimental data concerns the behavior of the spectra at around 5 eV. While the measurements in Ref. 7 found a plateau in absorption after the peak at 4 eV, in Refs. 21 and 74 a deep valley appears after 4 eV. All calculations we performed found a behavior qualitatively similar to the data reported in Ref. 21.

In Fig. 4 we compare results obtained within the RPA using scCOHSEX + G_0W_0 eigenvalues[77] and the ALDA using KS eigenvalues. The RPA curve obtained using KS eigenvalues overlaps almost perfectly with the ALDA curve. This proves that the inclusion of the ALDA kernel does not have any relevant effect on the absorption, as the important contributions due to electron-electron and electron-hole interactions are not accounted for by the ALDA kernel[38,48,78]. Both the RPA and the ALDA spectra using KS GGA eigenvalues are dramatically red-shifted.

We have also verified that an RPA spectrum that does not include local field effects is basically identical to an RPA spectrum with local field effects. If we now use the scCOHSEX + G_0W_0 eigenvalues for an RPA calculation [Fig. 4; dot-dashed (black) line], the resulting spectra are blue-shifted, while the line shape does not change. In fact, in the energy range of interest for absorption the *GW* correction is basically equivalent to application of a scissor operator. If we do a comparison with the experimental curves, the absorption peaks are now at energies that are too high. Additionally, the intensity of the RPA spectrum just above the onset appears underestimated. This is due to the neglect of excitonic effects within this approximation.

For many intermediate-gap semiconductors, it was shown[47–49] that the LRC to the xc kernel was enough to yield a good agreement with experimental absorption spectra. The LRC kernel works particularly well in the case of a continuum

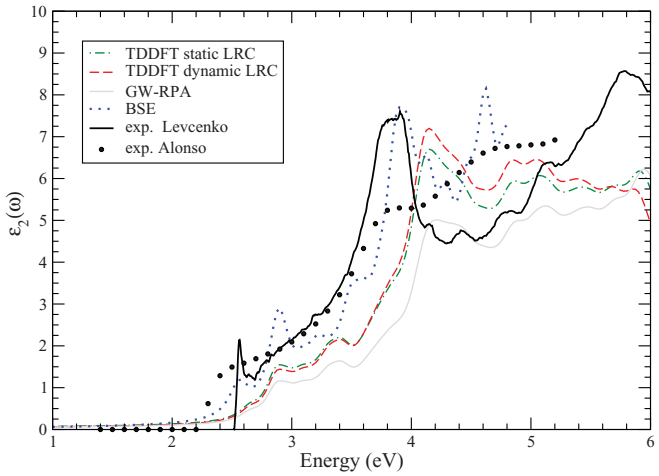

FIG. 5. (Color online) Imaginary part of the dielectric function for light polarized along the *c* axis obtained with the TDDFT using the static [dot-dashed (black) line] and the dynamic [dashed (red) line] LRC kernel, the GW-RPA [thin solid (gray) line], and the Bethe-Salpeter equation [dotted (blue) line], compared to experimental measurements of Alonso *et al.*[7] (filled circles) and Levcenko *et al.*[21] [thick solid (black) line; in arbitrary units].

exciton, giving, in general, very good optical properties with the efficiency of a TDDFT calculation. In Fig. 5 we show the spectra we obtained using the static[47,48] and the dynamic[49] versions of the LRC kernel. scCOHSEX + G_0W_0 eigenvalues were used in these calculations.

We extracted the parameter α^{static} required to define the static LRC kernel from theoretical quantities. More precisely, $\alpha^{\text{static}} = 0.37$ was obtained from the expression in Ref. 48 using the RPA value of the dielectric constant ε_∞ (7.9243). For the dynamical LRC, the expression in Ref. 49 leads to values of $\alpha^{\text{dyn}} = 0.11$ and $\beta = 0.004$. However, $CuGaS_2$has a bound exciton with strong effects on the spectrum, and in that case, the formula in Ref. 49 for the prediction of α^{dyn} and β may not be accurate. In fact, in order to obtain a reasonable spectrum for $CuGaS_2$, we need to use values of $\alpha^{\text{dyn}} = 0.11$ and $\beta = 0.02$, resorting to an empirical approach. The fact that local field effects are small gives us a hint of why the LRC kernel cannot modify much the spectrum.[79] Moreover, as the valence states involved are rather flat, one can expect that the LRC approximation is not enough to describe excitonic effects.

The TDDFT-LRC spectra shown in Fig. 5 provide a clear improvement with respect to the curves displayed in Fig. 4. The intensity of the peaks as well as the onsets of absorption are now closer to experiment. However, the peak at about 4 eV is still located at a higher energy than its experimental position. Note that the excitonic peak at the fundamental edge in $CuGaS_2$ has the nature of a bound exciton, even if the binding energy is rather low. This explains[48] why the LRC models do not reproduce the Bethe-Salpeter result perfectly. However, one should not forget that a TDDFT calculation using a model xc kernel is much less involved than a calculation which requires the solution of the BSE. In many cases, for example, when dealing with supercells with dopants, the best possible compromise, in terms of accuracy and computational costs, is clearly to perform calculations using model kernels derived from Bethe-Salpeter.

Of course, if one wants a reliable description of the bound excitonic peak of $CuGaS_2$,[10,21,26,27] it is advisable to resort to the solution of the BSE. Despite the fact that a shifted mesh of 1000 **k** points is not sufficiently dense to smooth out the curve, due to the strong dispersion of the lowest conduction state, the onset (at about 2.55 eV) and the peak (at about 3.8 eV) are already well converged (see Fig. 1) and they are in excellent agreement with experiments. At the absorption edge, we estimate an excitonic binding energy of about 0.1 eV, in agreement with experimental data.[11]

The peak at 3.8 eV is a resonant exciton coming from transitions between the two last valence bands and the first conduction band at **k** points in the region around the symmetry point *N*. The flatness of the bands in that region explains the large effect that the BSE has on this peak.

By comparing, in Fig. 6, the absorption for light polarized perpendicularly to the *c* axis or along the *c* axis, we can observe that the two experiments are once again in disagreement concerning the intensity of the absorption in the energy region of the peak at about 4 eV. All our calculations agree better in this case with the data of Alonso *et al.*[7] and predict a higher absorption for light polarized in the plane perpendicular to the *c* axis. The anisotropy of the optical response reflects an anisotropy of the band structure that is already present in the RPA spectra and is not significantly modified in the BSE result. The disagreement with the intensity of the polarization components of the spectra of Levcenko *et al.*[21] may, however, come from additional effects due to the way their absorption spectra were obtained. First, the polarization components when one measures reflectance may depend on the plane of growth of the samples [reflectances in Ref. 21 were measured in the (110) plane]. Second, it is well known[80,81] that extrapolation of the reflectance to the high-energy region (outside the range of the measurements) in order to apply the Kramers-Kronig relations affects the absolute value of the optical spectra. Finally, both experiments and our calculations agree that when light is polarized along the *c* axis, the absorption onset is at a slightly lower energy and the first excitonic peak is more pronounced.

Note that two other effects can contribute to the differences between experimental and theoretical onsets: the finite temperature of the experimental setup and, in the case of Ref. 7, a non-negligible amount of In in the samples. Both effects tend to close band gaps.

V. SUMMARY AND CONCLUSIONS

We used a state-of-the-art QPscGW approach to determine the electronic properties of $CuGaS_2$, which has been recognized as an ideal host semiconductor for intermediate-band thin-film solar cells. Perturbative GW is known to fail for Cu-based chalcopyrites, due to the *p-d* hybridization of the states forming the top of the valence band.[6] Indeed, this is also true for $CuGaS_2$: we found a G_0W_0 band gap almost 50% too small. An accurate band gap, in agreement with experimental data within 0.1 eV, was obtained using scCOHSEX + G_0W_0. In the energy range of interest for optical absorption the GW corrections shift the KS LDA bands almost rigidly, as we proved through the analysis of the effective masses, band widths, and relative positions of the conduction energy valleys.

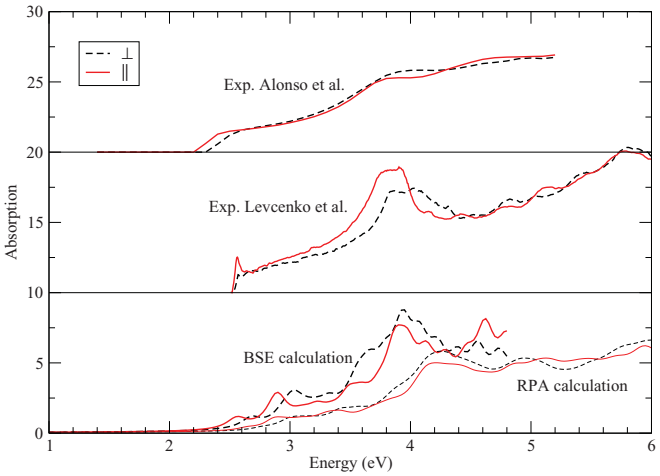

FIG. 6. (Color online) Comparison of BSE and GW-RPA absorption spectra with experimental absorption spectra from Refs. 7 and 21. Dashed (black) and solid (red) curves are results for light polarization perpendicular and parallel to the c axis, respectively.

This finding justifies the use of a scissor operator to correct the band gap. However, one should remember that the QP and LDA wave functions differ significantly for valence states close to the band gap, which are composed of hybridized s-p states.

We tested the importance of the inclusion of d states in the pseudopotential of Ga. We found that the differences in the GW gap are as small as 0.1 eV when including or excluding the 3 shell of Ga in the valence, which is the precision we can expect from a pseudopotential approach. The accuracy of GW results using the Ga pseudopotential without a semicore is then of the order of the difference between experimental results. This is important for reducing the computational costs in view of future calculations for $CuGaS_2$ doped with transition metals.

Regarding optical properties, the accuracy of RPA or ALDA *ab initio* calculations was not sufficient to explain the large discrepancies among experimental optical measurements. In view of this, we compared optical properties obtained with several theoretical levels of approximations. The simplest approaches, RPA or TDDFT with an ALDA kernel, using KS eigenvalues, yield a dramatic red-shift of the absorption spectra with respect to experiments, which reflects the strong underestimation of the gap in KS. The use of GW eigenvalues for a subsequent RPA calculation leads to spectra that are blue-shifted compared to experiments. This is due to the complete neglect of excitonic effects.

The inclusion of excitonic effects via the static and dynamical LRC kernel of the TDDFT improves the results: both the intensities of the peaks and the position of the absorption onset are significantly closer to experiments. However, the peak at about 4 eV still appears at higher energies than its experimental position and the bound excitonic peak at the fundamental edge is not reproduced. Only the solution of the BSE gives an accurate quantitative description of absorption. Nevertheless, we can conclude that the TDDFT can be an efficient and reliable alternative to the BSE, especially in view of calculations for large supercells, when the model LRC xc kernels derived from the BSEs are employed. Also, this conclusion is extremely relevant for further *ab initio* studies of doped systems, which require the use of large supercells, in order to describe the effect of the intermediate band on the optical absorption.

ACKNOWLEDGMENTS

This work was supported by the Consolider Ingenio 2010 Program, through project GENESIS-FV (reference no. CSD2006-04) of The Spanish Ministry of Education and Science, the NUMANCIA 2 project (S-2009ENE-1477) of the Comunidad de Madrid, and the EU Seventh Framework Programme under Grant Agreement No. 211956. The authors thankfully acknowledge the computer resources, technical expertise, and assistance provided by the Centro de Supercomputación y Visualización de Madrid (CeSViMa) and the Spanish Supercomputing Network. Some of the calculations were performed at IDRIS (Project Nos. x2010096017 and 09_544). I.A. would also like to thank the FOTOMAT project (MAT2009-14625-C03-01) for a research contract. S.B. acknowledges financial support from Programme PIR Matériaux–MaProSu No. 55744 of the CNRS. J.V. acknowledges support from the EDF/ANR CIFRE.

*silvana.botti@polytechnique.edu

[1] I. Repins, M. A. Contreras, B. Egaas, C. DeHart, J. Scharf, C. L. Perkins, B. To, and R. Noufi, Prog. Photovolt. **16**, 235 (2008).
[2] P. Jackson, D. Hariskos, E. Lotter, S. Paetel, R. Würz, R. Menner, W. Wischmann, and M. Powalla, Prog. Photovolt. Res. Appl., in press (2011), doi:10.1002/pip.1078.
[3] J. E. Jaffe and A. Zunger, Phys. Rev. B **29**, 1882 (1984).
[4] J. E. Jaffe and A. Zunger, Phys. Rev. B **27**, 5176 (1983).
[5] F. D. Jiang and J. Y. Feng, Semicond. Sci. Technol. **23**, 025001 (2008).
[6] J. Vidal, S. Botti, P. Olsson, J.-F. Guillemoles, and L. Reining, Phys. Rev. Lett. **104**, 056401 (2010).
[7] M. I. Alonso, K. Wakita, J. Pascual, M. Garriga, and N. Yamamoto, Phys. Rev. B **63**, 075203 (2001).
[8] J. L. Shay, B. Tell, H. M. Kasper, and L. M. Schiavone, Phys. Rev. B **5**, 5003 (1972).
[9] B. Tell, J. L. Shay, and H. M. Kasper, Phys. Rev. B **4**, 2463 (1971).
[10] C. Bellabarba, J. González, and C. Rincón, Phys. Rev. B **53**, 7792 (1996).
[11] N. N. Syrbu, I. M. Tiginyanu, L. L. Nemerenco, V. V. Ursaki, V. E. Tezlevan, and V. V. Zalamai, J. Phys. Chem. Solids **66**, 1974 (2005).
[12] J. R. Botha, M. S. Branch, P. R. Berndt, A. W. R. Leitch, and J. Weber, Thin Solid Films **515**, 6246 (2007).
[13] W. Shockley and H. J. Queisser, J. Appl. Phys. **32**, 510 (1961).
[14] D. F. Marrón, A. Martí, and A. Luque, Thin Solid Films **517**, 2452 (2009).
[15] I. Aguilera, P. Palacios, and P. Wahnón, Thin Solid Films **516**, 7055 (2008).

[16]P. Palacios, I. Aguilera, and P. Wahnón, Thin Solid Films **516**, 7070 (2008).
[17]P. Palacios, I. Aguilera, P. Wahnón, and J. C. Conesa, J. Phys. Chem. C **112**, 9525 (2008).
[18]A. Luque and A. Martí, Phys. Rev. Lett. **78**, 5014 (1997).
[19]A. Antolín, A. Martí, J. Olea, D. Pastor, G. González-Díaz, I. Mártil, and A. Luque, Appl. Phys. Lett. **94**, 042115 (2009).
[20]A. Martí, D. F. Marrón, and A. Luque, J. Appl. Phys. **103**, 073706 (2008).
[21]S. Levcenko, N. N. Syrbu, V. E. Tezlevan, E. Arushanov, S. Doka-Yamigno, T. Schedel-Niedrig, and M. C. Lux-Steiner, J. Phys. Condens. Matter **19**, 456222 (2007).
[22]C. Guillén and J. Herrero, Thin Solid Films **515**, 5917 (2007).
[23]S. Laksari, A. Chahed, N. Abbouni, O. Benhelal, and B. Abbar, Comput. Mater. Sci. **38**, 223 (2006).
[24]R. Ahuja, S. Auluck, O. Eriksson, J. M. Wills, and B. Johansson, Solar Energy Mater. Solar Cells **53**, 357 (1998).
[25]A. Soni, V. Gupta, C. Arora, A. Dashora, and B. Ahuja, Solar Energy **84**, 1481 (2010).
[26]B. Tell and H. M. Kasper, Phys. Rev. B **7**, 740 (1973).
[27]J. Ringeissen, J. L. Regolini, and S. Lewonczuk, Surface Sci. **37**, 777 (1973).
[28]S.-H. Wei and A. Zunger, Phys. Rev. B **37**, 8958 (1988).
[29]P. Hohenberg and W. Kohn, Phys. Rev. B **136**, 864 (1964).
[30]W. Kohn and L. J. Sham, Phys. Rev. A **140**, 1133 (1965).
[31]L. Hedin, Phys. Rev. A **139**, 796 (1965).
[32]E. E. Salpeter and H. A. Bethe, Phys. Rev. **84**, 1232 (1951).
[33]F. Aryasetiawan and O. Gunnarsson, Rep. Prog. Phys. **61**, 237 (1998).
[34]W. G. Aulbur, L. Jönsson, and J. W. Wilkins, Solid State Phys. **54**, 1 (1999).
[35]F. Bruneval, N. Vast, and L. Reining, Phys. Rev. B **74**, 045102 (2006).
[36]M. van Schilfgaarde, T. Kotani, and S. V. Faleev, Phys. Rev. Lett. **96**, 226402 (2006).
[37]T. Kotani, M. van Schilfgaarde, and S. V. Faleev, Phys. Rev. B **76**, 165106 (2007).
[38]G. Onida, L. Reining, and A. Rubio, Rev. Mod. Phys. **74**, 601 (2002), and refereces therein.
[39]S. Botti, A. Schindlmayr, R. Del Sole, and L. Reining, Rep. Prog. Phys. **70**, 357 (2007).
[40]M. Gatti, F. Bruneval, V. Olevano, and L. Reining, Phys. Rev. Lett. **99**, 266402 (2007).
[41]J. Vidal, F. Trani, F. Bruneval, M. A. L. Marques, and S. Botti, Phys. Rev. Lett. **104**, 136401 (2010).
[42]F. Trani, J. Vidal, S. Botti, and M. A. L. Marques, Phys. Rev. B **82**, 085115 (2010).
[43]S. V. Faleev, M. van Schilfgaarde, and T. Kotani, Phys. Rev. Lett. **93**, 126406 (2004).
[44]E. Runge and E. K. U. Gross, Phys. Rev. Lett. **52**, 997 (1984).
[45]E. K. U. Gross, F. J. Dobson, and M. Petersilka, *Density Functional Theory* (Springer, New York, 1996).
[46]A. Zangwill and P. Soven, Phys. Rev. A **21**, 1561 (1980).
[47]L. Reining, V. Olevano, A. Rubio, and G. Onida, Phys. Rev. Lett. **88**, 066404 (2002).
[48]S. Botti, F. Sottile, N. Vast, V. Olevano, L. Reining, H. C. Weissker, A. Rubio, G. Onida, R. Del Sole, and R. W. Godby, Phys. Rev. B **69**, 155112 (2004).
[49]S. Botti, A. Fourreau, F. Nguyen, Y.-O. Renault, F. Sottile, and L. Reining, Phys. Rev. B **72**, 125203 (2005).
[50]ABINIT code; [www.abinit.org].
[51]X. Gonze, J.-M. Beuken, R. Caracas, F. Detraux, M. Fuchs, G.-M. Rignanese, L. Sindic, M. Verstraete, G. Zerah, F. Jollet, M. Torrent, A. Roy, M. Mikami, P. Ghosez, J.-Y. Raty, and D. Allan, Comput. Mater. Sci. **25**, 478 (2002).
[52]X. Gonze, G.-M. Rignanese, M. Verstraete, J.-M. Beuken, Y. Pouillon, R. Caracas, F. Jollet, M. Torrent, G. Zerah, M. Mikami, P. Ghosez, M. Veithen, J.-Y. Raty, V. Olevano, F. Bruneval, L. Reining, R. Godby, G. Onida, D. Hamann, and D. Allan, Z. Kristallogr. **220**, 558 (2005).
[53]G. B. Bachelet, D. R. Hamann, and M. Schlüter, Phys. Rev. B **26**, 4199 (1982).
[54]N. Troullier and J. L. Martins, Phys. Rev. B **43**, 1993 (1991).
[55]D. R. Hamann, Phys. Rev. B **40**, 2980 (1989).
[56]M. Fuchs and M. Scheffler, Comput. Phys. Commun. **119**, 67 (1999).
[57]J. P. Perdew and Y. Wang, Phys. Rev. B **45**, 13244 (1992).
[58]R. W. Godby and R. J. Needs, Phys. Rev. Lett. **62**, 1169 (1989).
[59]J. Schneider, A. Rauber, and G. Brandt, J. Phys. Chem. Solids **34**, 443 (1973).
[60]S. C. Abrahams and J. L. Bernstein, J. Chem. Phys. **59**, 5415 (1973).
[61]H. Hahn, G. Frank, W. Klingler, A. Meyer, and G. Storger, Z. Anorg. Chem. **271**, 153 (1953).
[62]H. W. Spiess, V. Haeberln, G. Brandt, A. Rauber, and J. Schneider, Phys. Status Solidi B **62**, 183 (1974).
[63]M. S. Hybertsen and S. G. Louie, Phys. Rev. B **34**, 5390 (1986).
[64]W. Ku and A. G. Eguiluz, Phys. Rev. Lett. **89**, 126401 (2002).
[65]M. L. Tiago, S. Ismail-Beigi, and S. G. Louie, Phys. Rev. B **69**, 125212 (2004).
[66]K. Delaney, P. Garcia-Gonzalez, A. Rubio, P. Rinke, and R. W. Godby, Phys. Rev. Lett. **93**, 249701 (2004).
[67]C. Friedrich, A. Schindlmayr, S. Blügel, and T. Kotani, Phys. Rev. B **74**, 045104 (2006).
[68]A. Marini, G. Onida, and R. Del Sole, Phys. Rev. B **64**, 195125 (2001).
[69]F. Bruneval, N. Vast, L. Reining, M. Izquierdo, F. Sirotti, and N. Barrett, Phys. Rev. Lett. **97**, 267601 (2006).
[70]E. P. Domashevskaya, L. N. Marshakova, V. A. Terenkhov, A. N. Lukin, Y. A. Ugai, V. I. Nefedov, and Y. Y. Salyn, Phys. Status Solidi B **106**, 429 (1981).
[71]O. A. von Lilienfeld and P. A. Schultz, Phys. Rev. B **77**, 115202 (2008).
[72]A. Marini, C. Hogan, M. Grüning, and D. Varsano, Comput. Phys. Commun. **180**, 1392 (2009).
[73]M. Rohlfing and S. G. Louie, Phys. Rev. B **62**, 4927 (2000).
[74]J. C. Rife, R. N. Dexter, P. M. Bridenbaugh, and B. W. Veal, Phys. Rev. B **16**, 4491 (1977).
[75]A. Marini, G. Onida, and R. Del Sole, Phys. Rev. Lett. **88**, 016403 (2001).
[76]C. Persson, Appl. Phys. Lett. **93**, 072106 (2008).
[77]In practice, we verified that we can correct KS-GGA eigenvalues with a scissor operator of 1.7 eV. This allows us to match the scCOHSEX + G_0W_0 band structure in the energy range of interest for optical absorption.
[78]V. I. Gavrilenko and F. Bechstedt, Phys. Rev. B **55**, 4343 (1997).
[79]F. Sottile, F. Bruneval, A. G. Marinopoulos, L. K. Dash, S. Botti, V. Olevano, N. Vast, A. Rubio, and L. Reining, Int. J. Quantum Chem. **102**, 684 (2005).
[80]G. Leveque, J. Phys. C **10**, 4877 (1977).
[81]K. Jezierski, J. Phys. C **17**, 475 (1984).